Robust Fully-Connected PLL Network

Átila M. Bueno[(1)], José M. Balthazar[(2)],
Universidade Estadual Paulista.
Depto. de Estat. Mat. Aplic. e Comput. - DEMAC
Av. 24 A, 1515, Rio Claro, SP, Brazil, 13506-900
atila@lac.usp.br[(1)], jmbaltha@rc.unesp.br[(2)]

Diego P.F. Correa[(3)] and José R.C. Piqueira[(4)]
Universidade de São Paulo.
Depto. de Engenharia de Telecom. Controle - PTC
Av. Prof. L. Gualberto,tr3, 380, SP, Brazil, 05508-970
diego.correa@poli.usp.br[(3)], piqueira@lac.usp.br[(4)]

Abstract–Synchronization plays an important role in telecommunication systems and integrated circuits. The Master-Slave is a commonly used strategy for clock signal distribution. Recently, due to the wireless networks development and the higher operation frequency of integrated circuits, the Mutually-Connected clock distribution strategies are gaining importance and the Fully-Connected strategy appears as a convenient engineering solution. The Fully-Connected architecture complexity imposes difficulties to satisfy both stability and performance requirements in the control system design. For that reason the multi-variable LQG/LTR control technique is applied in attempting to fulfill both stability and performance requirements.The results seems to confirm the improvement in the transient response and in the precision of the clock distribution process.

Keywords: Synchronization; Phase-Locked Loop; Fully-Connected network; Robust Control.

I. INTRODUCTION

Synchronization allows the correct temporal order of information processing in communication systems, computation and control. The Master-Slave is a commonly used strategy for clock signal distribution [1, 2]. Recently, with the wireless networks development and the increase in the operation frequency of integrated circuits, the Fully-Connected clock distribution strategy is gaining importance (Fig.1). The Fully-Connected architecture is also being used in digital electronic circuits for clock signal distribution [3], and in synchronous neural networks for pattern recognition [4].

In a Fully-Connected architecture, the phase and frequency scales are determined by all the nodes. Differently from the Master-Slave strategies, the Fully-Connected presents a robust behavior when adding or dropping nodes. The nodes are build with PLLs (Fig.2) that are composed of a phase-detector (PD), a low-pass filter (f) and a voltage controlled oscillator (VCO)

[1, 2, 5]. The main drawback of the Fully-Connected architecture is the definition of control algorithms that can assure the stability of the network dynamic behavior [5, 6]. In hybrid synchronization techniques groups of nodes synchronized by the Fully-Connected architecture are synchronized with network master clocks by using the Master-Slave tecnique. In this arrangement, if a route of clock signal distribution becomes inoperative, the group of Fully-Connected nodes retain for some time the original phase and frequency received from the network [7].

The multi-variable linear quadratic gaussian and the loop transfer recovery (LQG/LTR) robust control techniques provide systematic procedures to design the compensator, and to analyse the dynamic stability of the system, besides robustness to a wide class of modelling errors [8, 6]. The technique is also suitable for this application due to multivariable characteristic of the Fully-Connected network. In section II the mathematical model of a Fully-Connected PLL network with N nodes is developed. The LQG/LTR robust control system design is shown in section III.
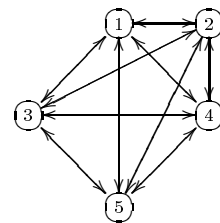

Figure 1: Fully-Connected architecture

II. MATHEMATICAL MODEL

For each node in a Fully-Connected PLL network,with N nodes, there are $N-1$ inputs to make the phase comparisons between the local VCO and the other nodes. There is also another phase comparison between the local VCO and the external input $v_I^{(j)}$, as shown in Fig. 2. The PDs outputs are weighted, generating the
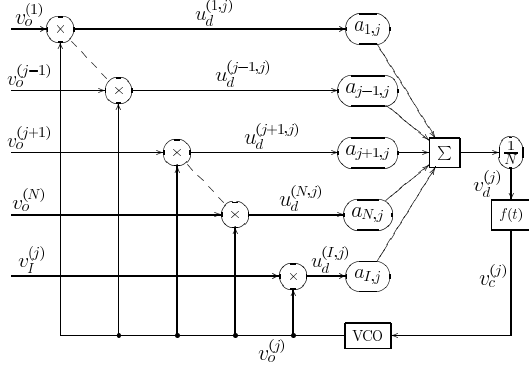
Figure 2: PLL block diagram

input to the filter $f^{(j)}(t)$, which feeds the local VCO.

The inputs and output signals are given by:

$$v_I^{(j)}(t) = \mathrm{v}_I^{(j)} \sin\left(\omega_M t + \theta_I^{(j)}(t)\right), \qquad (1)$$

and

$$v_o^{(j)}(t) = \mathrm{v}_o^{(j)} \cos\left(\omega_M t + \theta_o^{(j)}(t)\right), \qquad (2)$$

where v_I and v_o are the amplitudes of the input and output signals, and ω_M is the free-running frequency of all VCOs. The coupling between the nodes is carried out by an inner coupling input, given by:

$$v_o^{(\ell)}(t) = \mathrm{v}_o^{(\ell)} \sin\left(\omega_M t + \theta_o^{(\ell)}(t)\right), \qquad (3)$$

for $\ell = 1, \ldots, j-1, j+1, \ldots, N$,

The filter is all-pole [2] with transfer function given by:

$$F(s) = \frac{\alpha_0}{s + \beta_0}. \qquad (4)$$

The weighted PDs output is:

$$v_d^{(j)}(t) = \frac{1}{N}\left[\sum_{\substack{\ell=1 \\ \ell \neq j}}^{N} \frac{k^{(\ell,j)}}{k_o^{(j)}} \sin\left(\theta_o^{(\ell)}(t) - \theta_o^{(j)}(t)\right) + \right.$$
$$\left. \frac{k^{(I,j)}}{k_o^{(j)}} \sin\left(\theta_I^{(j)}(t) - \theta_o^{(j)}(t)\right) \right], \quad (5)$$

with the loop gains given by:

$$k^{(\ell,j)} = \frac{1}{2} a_{\ell,j} k_m^{(j)} k_o^{(j)} \mathrm{v}_o^{(j)} \mathrm{v}_o^{(\ell)}, \qquad (6)$$

$$k^{(I,j)} = \frac{1}{2} a_{I,j} k_m^{(j)} k_o^{(j)} \mathrm{v}_o^{(j)} \mathrm{v}_I^{(j)}, \qquad (7)$$

where $k_m^{(j)}$ is the PD gain, $k_o^{(j)}$ the VCO gain, $a_{\ell,j}$ and $a_{I,j}$ are the PDs weighting factors. In (5) the double-frequency terms are neglected because they are supposed to be filtered [5].

The output of the VCO is controlled according to the relation:

$$\frac{d}{dt}\theta_o^{(j)}(t) = k_o^{(j)} v_c^{(j)}(t), \qquad (8)$$

where

$$v_c^{(j)}(t) = \int_0^t f^{(j)}(t-\tau) v_d^{(j)}(\tau) d\tau. \qquad (9)$$

In order to simplify the mathematical reasoning all the constitutive parameters of the nodes are considered to be the same, then, $k^{(\ell,j)} = k^{(I,j)} = k$. Considering the former relations and applying the convolution theorem [10] the dynamics of the phase output of the nodes is given by:

$$\ddot{\theta}_o^{(j)} + \beta_0 \dot{\theta}_o^{(j)} - \alpha_0 \frac{k}{N}\left[\sum_{\substack{\ell=1 \\ \ell \neq j}}^{N} \sin\left(\theta_o^{(\ell)} - \theta_o^{(j)}\right) + \right.$$
$$\left. \sin\left(\theta_I^{(j)} - \theta_o^{(j)}\right) \right] = 0, \quad (10)$$

for $j = 1, 2, \ldots, N$. Additionaly, for small phase errors, the sinusoids in (10) can be simplyfied by using the first terms in the Taylor's series [10, 11, 5], resulting:

$$\ddot{\theta}_o^{(j)} + \beta_0 \dot{\theta}_o^{(j)} + \alpha_0 k \left[\theta_o^{(j)} + \frac{1}{N} \sum_{\substack{\ell=1 \\ \ell \neq j}}^{N} \theta_o^{(\ell)} \right] = \alpha_0 k \theta_I^{(j)}, \quad (11)$$

for $j = 1, 2, \ldots, N$, which can be tranformed into state space equations by defining the state variables as follows:

$$\begin{aligned} x_1^{(j)} &= \theta_o^{(j)} \\ x_2^{(j)} &= \dot{\theta}_o^{(j)} \end{aligned} \qquad (12)$$

resulting,

$$\dot{x}_1^{(j)} = x_2^{(j)} \qquad (13)$$
$$\dot{x}_2^{(j)} = -\beta_0 x_2^{(j)} - \alpha_0 k \left[x_1^{(j)} + \frac{1}{N} \sum_{\substack{\ell=1 \\ \ell \neq j}}^{N} x_1^{(\ell)} \right] + \alpha_0 k \theta_I^{(j)},$$

for $j = 1, 2, \ldots, N$.

III. LQG/LTR Control system design

As an example, the multivariable Fully-Connected network is implemented consisting of two nodes ($N = 2$), i.e., two external inputs - see (1) - and two outputs. The other parameters are set in order to generate a stable Fully-Connected network [5]. The loop-gain is set to $k = 1$ and the filter coefficients are set to $\alpha_0 = 0.6283$ and $\beta_0 = 0.6283$. Accordingly the state space equation for this network is given by:

$$\dot{\mathbf{x}}_\mathbf{n} = \mathbf{A}_\mathbf{n}\mathbf{x}_\mathbf{n} + \mathbf{B}_\mathbf{n}\mathbf{u}_\mathbf{n} \qquad (14)$$
$$\mathbf{y}_\mathbf{n} = \mathbf{C}_\mathbf{n}\mathbf{x}_\mathbf{n} + \mathbf{D}_\mathbf{n}\mathbf{u}_\mathbf{n}. \qquad (15)$$

2

with $\mathbf{D_n} = \mathbf{0}_{2\times2}$, $\mathbf{x_n} = \begin{bmatrix} x_1^{(1)} & x_2^{(1)} & x_1^{(2)} & x_2^{(2)} \end{bmatrix}^T$ and $\mathbf{u_n} = \begin{bmatrix} \theta_I^{(1)} & \theta_I^{(2)} \end{bmatrix}^T$. For a precise clock signal distribution the network needs to track phase steps with null steady state error. For that reason pure integrators must be added to the loop, resulting that the nominal system transfer function matrix is given by:

$$\mathbf{G_N}(s) = \mathbf{C}(s\mathbf{I} - \mathbf{A})^{-1}\mathbf{B} \qquad (16)$$

where $\mathbf{A} = \begin{bmatrix} \mathbf{0}_{2\times2} & \mathbf{C_n} \\ \mathbf{B_n} & \mathbf{A_n} \end{bmatrix}$, $\mathbf{B} = \begin{bmatrix} \mathbf{I}_{2\times2} \\ \mathbf{0}_{4\times2} \end{bmatrix}$ and $\mathbf{C} = \begin{bmatrix} \mathbf{0}_{2\times2} & \mathbf{C_n} \end{bmatrix}$. In addition, $\mathbf{x} = \begin{bmatrix} \mathbf{u_n}^T & \mathbf{x_n}^T \end{bmatrix}^T$ [8].

The transfer function matrix is a multivariable state space description of the nominal network. In this case, the frequency response of the system is given in terms of the singular values of the transfer function matrix [8, 9]. The transfer function matrix has two singular values denoted respecively by $\sigma_M(\mathbf{G_N})$ and $\sigma_m(\mathbf{G_N})$, where M stands for maximun and m for minimum.

The stability analysis of multivariable systems is done by means of its stability barrier, wich is a function of ω. All singular values of the frequency response must be located bellow this barrier. The stability barrier is obtained from the error matrices generated by all possible combinations of deviations. The error matrix is defined as:

$$\epsilon(j\omega) = [\mathbf{G_R}(j\omega) - \mathbf{G_N}(j\omega)]\,\mathbf{G_N}^{-1}(j\omega) \qquad (17)$$

where $\mathbf{G_R}(s)$ is the real system transfer function matrix [8, 9, 6], and the stability barrier is defined by:

$$b(\omega) = \frac{1}{e_M(\omega)} \qquad (18)$$

where $e_M(\omega) = max\,[\sigma_M(\epsilon(j\omega))]$. The stability barrier is determined, using MATLAB [12], for 300 values of ω, in the range of interest, and for combinations of the deviations of the filter coefficients, α_0 and β_0.

The performance requirements are accomplished by the disturbance rejection barrier ($\alpha_n(\omega)$) and by the reference tracking barrier ($p(\omega)$). In the case of disturbance rejection barrier both open loop and closed loop singular values must be bellow the barrier. On the other hand, in the case of reference tracking barrier, the open loop singular values must be above the barrier [8, 9, 6]. The robustness barriers are shown in Fig. 3. Clearly, the frequency response of the uncompensated nominal system $\mathbf{G_N}(s)$, shown in Fig. 3, do not satisfy the stability barrier.

The LQG/LTR method is used to design the closed loop control system with the compensator $\mathbf{K}(s)$, as shown in Fig.4. The LQG/LTR is applied following the steps.

- The "target loop" transfer function matrix $\mathbf{G_{TL}}$ is determined according to $\mathbf{G_{TL}}(s) = $
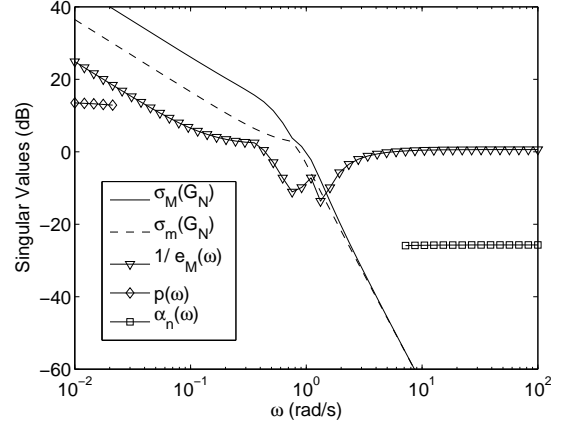

Figure 3: Nominal system singular values and robustness barriers

$\frac{1}{\mu}\mathbf{C}\,(s\mathbf{I} - \mathbf{A})^{-1}\mathbf{L}$, where μ and $\mathbf{L}$ are chosen in order to satisfy $\sigma_M(\mathbf{G_{TL}}(j\omega)) < b(\omega)$ at high frequencies. Here $\mathbf{L}$ was determined using the Cabral criterion [8].

- The state observer gain matrix is determined by $\mathbf{H} = \frac{1}{\mu}\mathbf{\Sigma}\mathbf{C}^T$, where $\mathbf{\Sigma}$ is the solution of the algebraic Riccati equation: $\mathbf{A}\mathbf{\Sigma} + \mathbf{\Sigma}\mathbf{A}^T + \mathbf{L}\mathbf{L}^T - \frac{1}{\mu}\mathbf{\Sigma}\mathbf{C}^T\mathbf{C}\mathbf{\Sigma} = \mathbf{0}$.

- The state regulator gain matrix is determined by $\mathbf{G} = \frac{1}{\rho}\mathbf{B}^T\mathbf{\Phi}$, where $\mathbf{\Phi}$ is the solution of another algebraic Riccati equation: $-\mathbf{\Phi}\mathbf{A} - \mathbf{A}^T\mathbf{\Phi} - \mathbf{C}^T\mathbf{C} + \frac{1}{\rho}\mathbf{\Phi}\mathbf{B}\mathbf{B}^T\mathbf{\Phi} = \mathbf{0}$. The parameter ρ is a small positive number that matches the frequency response of the whole system to the target loop.

- The compensator matrix transfer function is given by $\mathbf{K}(s) = \mathbf{G}\,[s\mathbf{I} - (\mathbf{A} + \mathbf{B}\mathbf{G} + \mathbf{H}\mathbf{C})]^{-1}\mathbf{H}$.

The compensator $\mathbf{K}(s)$ can be implemented by active or passive synthesis of networks, and the matrix $\mathbf{G_N}(s)\mathbf{K}(s)$ satisfy both $\sigma_M(\mathbf{G_N}(j\omega)\mathbf{K}(j\omega)) < b(\omega)$ and $\sigma_M(\mathbf{C_N}) < b(\omega)$, where $\mathbf{C_N}$ is the closed loop matrix transfer function of the compensated system, given by:

$$\mathbf{C_N}(s) = [\mathbf{I} + \mathbf{G_N}(s)\mathbf{K}(s)]^{-1}\mathbf{G_N}(s)\mathbf{K}(s), \qquad (19)$$

assuring the stability of the system. Finally, as shown in Fig. 5, the singular values of both the open loop and closed loop system satisfy the robustness barriers.

The performace of the compensated Fully-Connected network can be seen in Figs. 6 and 7. In Fig. 6 both uncompensated and compensated networks are compared, the compensated network presents null steady state error to a step input in θ_I^1. In Fig. 7 the compensated network rejects the double-frequency jitter (DFJ) [13], applied as a disturbance $\mathbf{d}(s)$ (see Fig. 4). The DFJ is attenuated at a rate of $-60dB$ approximately.
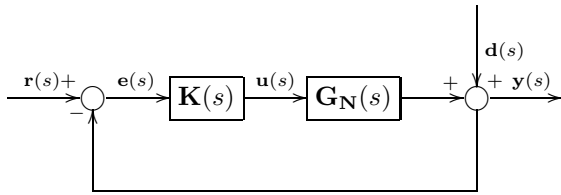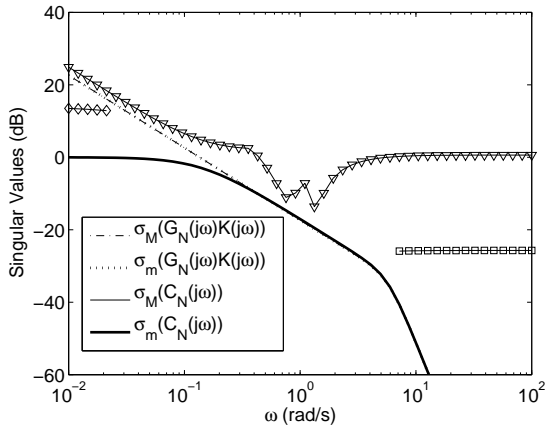
3

Figure 4: Control system block diagram

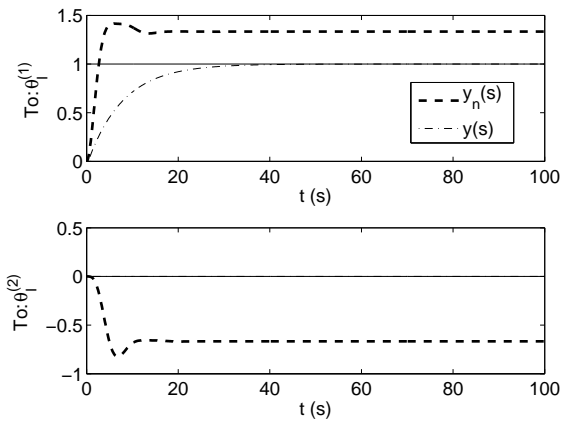Figure 5: Open loop and closed loop singular values

Figure 6: Step response

IV. Conclusion

The proposed Fully-Connected network is suitable to generate clock signals to be distributed in a hybrid synchronization technique. The multivariable LQG/LTR was used in the analysis and to assure stability even in the presence of modelling errors. Also the tolerance to jitter was observed, with the DFJ applied as a disturbance. The attenuation to the DFJ is of $-60dB$, which can be considered satifactory. Accordingly, Fully-Connected networks with phase weighting PDs implemented with LQG/LTR control technique
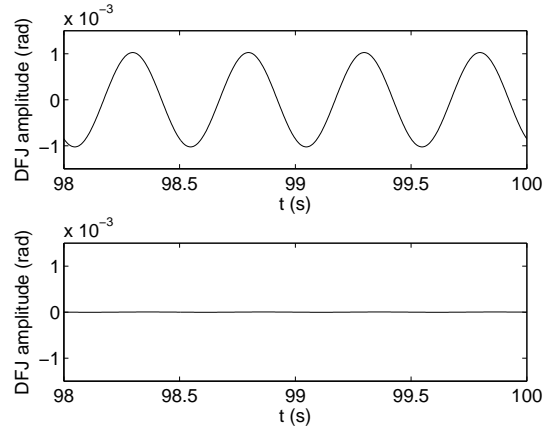

Figure 7: Response to double-frequency jitter (DFJ)

can increase the reliability and quality of the clock signal distribution in telecommunication networks.

References

[1] W. C. Lindsey, F. Ghazvinian, W. C. Hagmann, and K. Dessouky. Network synchronization. In *Proceedings of the IEEE*, volume 73, pages 1445–1467, Oct. 1985.

[2] J. R. C. Piqueira and L. H. A. Monteiro. All-pole phase-locked loops: calculating lock-in range by using evan's root-locus. *International Journal of Control*, 79(07):822–829, July 2006.

[3] M. Saint-Laurent and M. Swaminathan. A multi-pll clock distribution architecture for gigascale integration. In *Proceedings. IEEE Computer Society Workshop on VLSI, 2001.*, pages 30–35, 2001.

[4] M. K. S. Kunyosi and L. H. A. Monteiro. Recognition of noisy images by pll networks. *Signal Processing*, 89(7):1311–1319, 2009.

[5] A. M. Bueno, A. A. Ferreira, and J. R. C. Piqueira. Fully connected pll networks: How filter determines the number of nodes. *Mathematical Problems In Engineering*, 2009.

[6] R. B. Pinheiro, J. J. Da Cruz, and J. R. C. Piqueira. Robust clock generation system. *International Journal of Control*, 80(1):35–44, Jan. 2007.

[7] H. Yahata. Hybrid clock synchronization: The pull-in range of a ring network. *Electronics and Communications In Japan Part I-Communications*, 82(6):45–59, June 1999.

[8] J. J. Da Cruz. *Controle Robusto Multivariável*, volume 1. Edusp, 1 edition, 1996.

[9] J. Doyle and G. Stein. Multivariable feedback design - concepts for a classical-modern synthesis. *Ieee Transactions On Automatic Control*, 26(1):4–16, 1981.

[10] T. Kailath. *Linear Systems*. Prentice-Hall information and system science series. Englewood Cliffs, N.J. : Prentice-Hall, 1980.

[11] J. Guckenheimer and P. Holmes. *Nonlinear Oscillations, Dynamical Systems, and Bifurcations of Vector Fields*, volume 42 of *Applied Mathematical Sciences*. Springer, 2 edition, 1983.

[12] S. Lynch. *Dynamical Systems With Applications Using MATLAB*. Birkhauser, Boston, 1 edition, 2004.

[13] A. A. Ferreira, A. M. Bueno, and J. R. C. Piqueira. Modeling and measuring double-frequency jitter in one-way master-slave networks. *Communications In Nonlinear Science and Numerical Simulation*, 14(5):1854–1860, May 2009.